Local-structure origins of the sustained Curie temperature in (Ba,Ca)TiO3 ferroelectrics

Igor Levin, Victor Krayzman, and Joseph C. Woicik

Additional information on Appl. Phys. Lett.

Local-structure origins of the sustained Curie temperature in (Ba,Ca)TiO$_3$ ferroelectrics

Igor Levin,[1] Victor Krayzman,[1,2] and Joseph C. Woicik[1]

[1]*Materials Measurement Science Division, National Institute of Standards and Technology, Gaithersburg, Maryland 20899, USA*

[2]*Department of Materials Science & Engineering, University of Maryland, College Park, Maryland 20742, USA*

While the lattice volume in the solid-solution Ba$_{1-x}$Ca$_x$TiO$_3$ decreases with increasing x, the Curie temperature remains unaffected, in contrast to Ba$_{1-x}$Sr$_x$TiO$_3$. We have determined the origin of this phenomenon by comparing the local structures in (Ba,Ca)TiO$_3$ and (Ba,Sr)TiO$_3$. Reverse Monte Carlo refinements of instantaneous atomic positions using simultaneous fitting of multiple types of experimental data (neutron total scattering, X-ray absorption fine structure, patterns of diffuse scattering in electron diffraction) reveal both ferroelectric Ca displacements and their amplification of the Ti off-centering, which mitigate the lattice-volume effects. The activity of Ca is triggered by the anomalously strained Ca-O bonds. © 2013 AIP Publishing LLC
[http://dx.doi.org/10.1063/1.4802996]

BaTiO$_3$ (BT), a classical perovskite-like ferroelectric,[1] serves in many key commercial applications. BT exhibits a series of polymorphic phase transitions cubic ↔ tetragonal ↔ orthorhombic ↔ rhombohedral.[1–3] The high-temperature cubic phase is paraelectric, whereas all low-temperatures polymorphs are ferroelectric. The Ti cations, 6-fold coordinated by oxygen, are locally off-centered even in the cubic structure, which exhibits rhombohedral-like distortions of the [TiO$_6$] octahedra.[4–6] These distortions are retained in all of the ferroelectric polymorphs.[6]

Usually, a set of properties required for a particular application is achieved by chemical substitutions on the Ba (ionic radius[7] R = 1.61 Å) and/or Ti (R = 0.60 Å) sites. Strontium (R = 1.44 Å) and calcium (R = 1.34 Å) are common Ba-site constituents in practical BT-based systems. BaTiO$_3$ and SrTiO$_3$ form continuous (Ba,Sr)TiO$_3$ (BST) solid solutions.[8] In contrast, BT and CaTiO$_3$ (CT) are only partially miscible with solubility on either side of the BT-CT (BCT) diagram limited to ≈20 mol. % at 1450 °C.[9] In BST, the Curie temperature (T_C) decreases continuously as the Sr content increases.[10] Intriguingly, in BCT, the T_C remains approximately constant up to the solubility limit of Ca.[11,12]

Despite the fundamental and commercial importance of BT-based systems, the origin of a counterintuitive difference between the effects of Sr and Ca on T_C remains unclear. Earlier speculative arguments[13] and recent theoretical calculations[12] suggested that polar Ca displacements stabilize the tetragonal phase; however, no experimental information on the local structure in BCT solid solutions has been reported. Furthermore, existing explanations ignore the effect of Ba-site substitutions on the Ti off-centering, which is a key feature of the ferroelectric behavior in BT. Crystal chemistry attributes this off-centering to a relatively large volume of the [TiO$_6$] octahedron, which in turn is determined by the large ionic radius of Ba. Indeed, according to variable-pressure studies, local Ti off-centering in BT is suppressed by the decreasing unit-cell volume (V_o).[14,15] Substitution of smaller cations (i.e., Sr, Ca) on the A-sites in BT also

reduces V_0 and, consequently, the average octahedral volume ($1/6V_0$). Shrinkage of octahedral volumes with increasing Sr content is commonly used to explain the behavior of T_C in BST. If such volume effects were also dominant in BCT, this system would feature an even stronger suppression of T_C-a prediction that contradicts the experimental observations.[11,12]

The goal of the present study was to establish differences in the local structure of BST and BCT solid solutions that are responsible for the distinct effects of Sr and Ca on the macroscopic polarization (P_s) and, therefore, on the Curie temperature ($T_C \propto P_s^2$ [Ref. 1]). We resolve this decades-old controversy by using the structure-refinement technique that involves simultaneous fitting of an atomistic structural model to several types of experimental data. This technique enables explicit determination of instantaneous atomic positions with the accuracy and detail inaccessible by single-technique analyses. According to our results, Ca atoms in the large Ba-site cavities of BT are ferroelectrically active and contribute to polarization both through their own polar displacements and by promoting the local Ti off-centering, as does Pb in PbTiO$_3$. The ferroelectric activity of Ca is supported by the highly strained Ca-O and Ba-O bonds, which contrast with the significantly more relaxed Sr-O and Ba-O bonds in BST. In BCT, local Ti displacements are aligned much closer with the tetragonal axis than those in BT and BST, which further enhances the polarization.

We analyzed ceramic samples of Ba$_{1-x}$Sr$_x$TiO$_3$ ($x = 0$, 0.05, 0.1, 0.2, 0.5) and Ba$_{1-x}$Ca$_x$TiO$_3$ ($x = 0.05$, 0.1, 0.2, 0.3), prepared using conventional solid-state synthesis.[16] Ambient-temperature X-ray diffraction patterns confirm that BST ($x < 0.5$), and BCT ($x \le 0.3$)[17] are tetragonal, whereas BST ($x = 0.5$) is cubic. The unit-cell volume shrinks continuously with increasing concentrations of Sr and Ca; the decrease is larger for Ca as expected from its smaller ionic radius (Fig. 1(a)). In BST, the c/a ratio and T_C decrease linearly with increasing x, while in BCT, both parameters remain approximately constant (Fig. 1(b)).
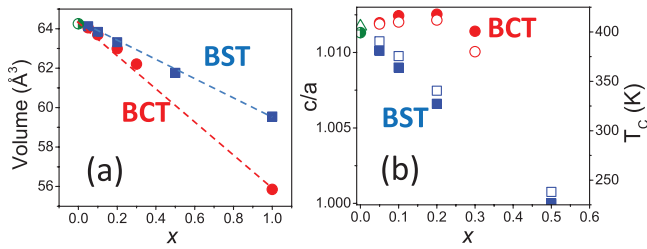
FIG. 1. Compositional dependence of the (a) unit-cell volume and (b) c/a ratio (filled symbols) and T_C (open symbols) in the BST (blue) and BCT (red) solid solutions, as determined using XRD. The data points for BT are indicated in green.

FIG. 2. (a) XAS Ti K near-edge structure in $Ba_{1-x}Sr_xTiO_3$ (1: $x=0$, 2: $x=0.2$, 3: $x=0.5$, 4: $x=1.0$) and $Ba_{1-x}Ca_xTiO_3$ (5: $x=0.2$, 6: $x=0.3$). Inset: a magnified view of the pre-edge peak related to the Ti off-centering (δ_{Ti}). (b) δ_{Ti} determined from the intensity of the pre-edge peak as a function of the unit-cell volume in BT (green half-filled circle), BST (blue squares), and BCT (red circles). The value of δ_{Ti} for $CaTiO_3$ (labeled 7) was determined using the spectrum reported in Ref. 20.

TABLE I. Contributions to polarization P_s (in C/m^2) from individual crystallographic sites as calculated from the presently refined atomic coordinates and Born effective charges.[19] The z-coordinate of the apical O atoms is fixed at zero. The equatorial oxygen atoms are labeled as O_{eq}. The changes in T_c relative to that in $BaTiO_3$ (T_c^*) are calculated according to $T_c \propto P_s^2$ relationship, where the same proportionality constant is assumed for all compositions.

Composition	A-site	Ti-site	O_{eq}	P_s	T_c/T_c^*
$BaTiO_3$	0.072	0.271	-0.048	0.295	1.00
$Ba_{0.8}Ca_{0.2}TiO_3$	0.081	0.257	-0.030	0.308	1.09
$Ba_{0.7}Ca_{0.3}TiO_3$	0.074	0.271	-0.023	0.322	1.19
$Ba_{0.8}Sr_{0.2}TiO_3$	0.064	0.202	-0.032	0.234	0.63

Rietveld refinements[18] of the average tetragonal structures of BT, BST ($x=0.2$), and BCT ($x=0.2, 0.3$) were performed in space group $P4mm$ using neutron powder diffraction data.[16] The refined atomic coordinates were used to evaluate the individual site contributions to the net polarization (Table I). The effects of Ca and Sr substitution on T_C (Table I) reproduce the experimental T_C trends satisfactorily (Fig. 1(b)). Calcium substitution enhances the A-site contribution to P_s with a larger increase observed for smaller Ca concentrations. The B-site contribution is diminished for all the solid-solution samples, but the decrease is much smaller for BCT compared to BST. Clearly, the polarization of BCT is sustained to a large degree because of the influence of Ca on the Ti off-centering along the c-axis. These results contradict the current perception, which attributes all of the effect to ferroelectric Ca displacements.

Local Ti off-centering is manifested in the Ti K pre-edge peak in X-ray absorption spectra (XAS)[5] (Fig. 2(a)). The integrated intensity of this peak (Fig. 2(b)) is directly proportional to the mean-squared displacements of Ti (δ_{Ti}) off the instantaneous centers of oxygen octahedra.[5] Note that δ_{Ti} represents the off-centering of Ti relative to O, which should not be confused with Ti displacements. Previous studies of ceramic and single-crystal $BaTiO_3$ yielded $\delta_{Ti} = 0.23(1)$ Å.[6] We adopted this value as a reference for calculating local Ti off-centering from the pre-edge peak intensities in the solid-solution samples (Fig. 2(b)). Clearly, the local value of δ_{Ti} in BCT is also larger than that expected from the relatively small unit-cell volume.

Thus, understanding the effects of Ca substitution on P_s requires answers to the following questions: (1) Why do $Ba_{0.7}Ca_{0.3}TiO_3$ and $Ba_{0.8}Sr_{0.2}TiO_3$ exhibit similar local Ti off-centering despite a significantly smaller unit-cell volume
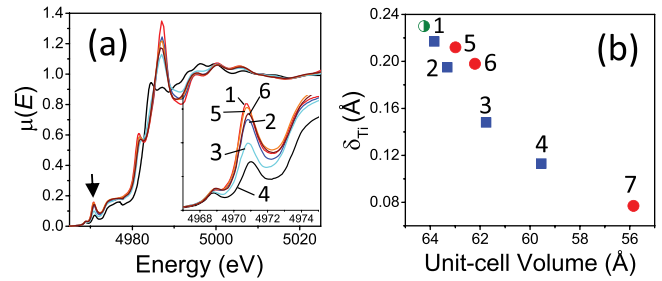
in $Ba_{0.7}Ca_{0.3}TiO_3$, and (2) why does $Ba_{0.7}Ca_{0.3}TiO_3$ exhibit a much larger *average* Ti off-centering (along the c-axis) than $Ba_{0.8}Sr_{0.2}TiO_3$, given the similar *local* Ti off-centering in both structures?

We reconciled local and average displacements/distortions by performing *simultaneous* fitting of several types of experimental data using a Reverse Monte Carlo (RMC) algorithm implemented in the RMCProfile software.[16,20–23] The following data were included in the fit: (1) real-space pair-distribution function (PDF) as determined from the neutron total-scattering, (2) reciprocal-space neutron total-scattering function S(Q), (3) neutron Bragg intensities, (4) patterns (not intensities) of electron diffuse scattering measured from single-crystal grains of the ceramic samples, (5) EXAFS (Ca K edge for BCT and Sr K edge for BST), (6) magnitude of the local Ti off-centering as deduced from the Ti K pre-edge peak, and (7) macroscopic value of polarization. (The polarization values calculated from the average atomic coordinates, Table I, were adopted.) All these complementary data are critical for constraining the atomic configurations because fitting *any* of the data subsets cannot reproduce other experimental results, thus yielding an obviously incorrect structure.[24] RMC fits produced a good agreement between the experimental and calculated signals for all the datasets (Fig. 3). The refined configurations were analyzed to determine key local-structure features that contribute to a macroscopic polarization.

The probability density distribution (PDD) for Ti in BT (Fig. 4(a)) is consistent with a 4-site model proposed previously.[4] These sites are closely spaced and visually unresolved in the (001)-projected PDD maps. However, the PDD profiles along $\langle 110 \rangle$ directions exhibit broad tops (Fig. 4(a)), as expected for a 4-site distribution. The Ti PDD in $Ba_{0.8}Sr_{0.2}TiO_3$ is qualitatively similar to that for BT, but with a smaller site splitting (Fig. 4(b)). In contrast, the Ti PDD in $Ba_{0.7}Ca_{0.3}TiO_3$ (Fig. 4(c)) is much narrower and definitely unimodal. Indeed, Ti displacements in $Ba_{0.7}Ca_{0.3}TiO_3$ are aligned closely with the c-axis, which contrasts with significant deviations observed in both BT ($\approx 20°$) and $Ba_{0.8}Sr_{0.2}TiO_3$ ($\approx 30°$).[25] (In all three samples, the Ti displacements exhibit detectable preference for the (110) planes.) The ratio of the c- and a-axis components of δ_{Ti} is also considerably larger for $Ba_{0.7}Ca_{0.3}TiO_3$; thus, the local distortion of
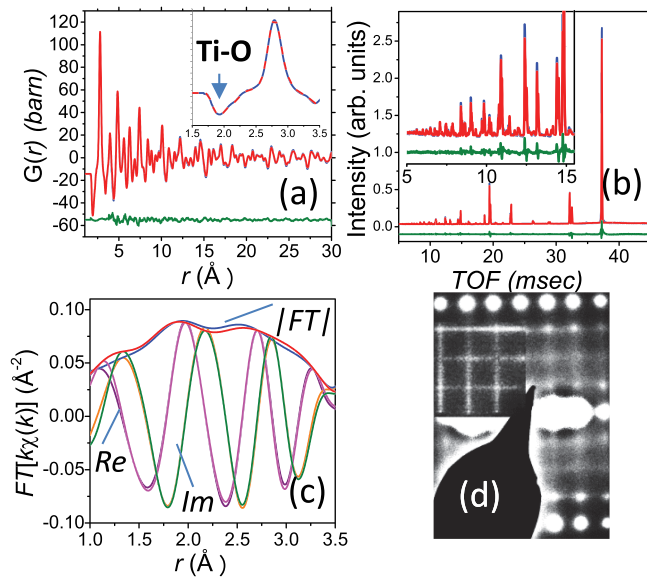
FIG. 3. Experimental (red) and calculated (blue) patterns for the (a) neutron $G(r)$, (b) neutron Bragg profile, (c) Ca EXAFS, and (d) electron diffuse scattering (reciprocal-lattice section (014)*) in $Ba_{0.7}Ca_{0.3}TiO_3$ (the calculated pattern is shown in the upper left quadrant as an inset). For EXAFS, the real and imaginary parts of the signal (weighted by k) Fourier transform (FT) are shown in addition to the total magnitude. The k-range used in the FT was from $k = 2.8\,\text{Å}^{-1}$ to $k = 9.5\,\text{Å}^{-1}$. The Ca-O, Ca-Ti, and Ca-Ca, single-scattering paths were included in the EXAFS fit. The values of δ_{Ti} and P_s for the refined configuration matched the experimental values. Similar-quality fits were obtained for the $BaTiO_3$ and $Ba_{0.8}Sr_{0.2}TiO_3$ samples.

$[TiO_6]$ coordination in $Ba_{0.7}Ca_{0.3}TiO_3$ is tetragonal-like. This explains why despite similar magnitudes of the *total* Ti off-centering in $Ba_{0.8}Sr_{0.2}TiO_3$ and $Ba_{0.7}Ca_{0.3}TiO_3$, the c-axis component of this off-centering, which contributes to P_s, is significantly larger in $Ba_{0.7}Ca_{0.3}TiO_3$ (Fig. 2). Note that all three refined structures (BT, BST, BCT) featured extended linear correlations of the x- and y-axis components of Ti displacements along the [100] and [010] chains, respectively, as manifested by the $\{100\}^*$ diffuse-scattering sheets in electron diffraction patterns (Fig. 3(d)).

Strontium displacements provide little additional contribution to P_s of $Ba_{0.8}Sr_{0.2}TiO_3$, as reflected in the similar average z-coordinates of the Sr and Ba atoms ($z_{Sr} = 0.012$, $z_{Ba} = 0.013$). The average Sr-O distance (2.78 Å) is appreciably shorter than the average Ba-O (2.83 Å) distance and similar to the Sr-O distance in $SrTiO_3$ (2.76 Å). The average Ba-O distances in $Ba_{0.8}Sr_{0.2}TiO_3$ and $BaTiO_3$ nearly coincide. Fitting the 1st peaks in the Sr-O and Ba-O partial PDFs (obtained from the RMC refinements) using parameterized models[16] confirmed that the distortions of the average

$[SrO_{12}]$ and $[BaO_{12}]$ cube-octahedra are relatively small with the shortest Sr-O distances of ≈ 2.64 Å ($\times 4$). The bond valence sum (BVS)[26,27] for Sr is 2.4, which indicates that the Sr-O tensile bond strain is completely relieved, while the BVS for Ba is 2.8, similar to BT. In the coordination groups $[TiO_6Ba_{8-N}Sr_N]$, which include both the nearest and the next-nearest Ti neighbors, octahedral volumes (V_{oct}) shrink and Ti off-centering is suppressed with increasing N (Fig. 5(a)), thereby explaining linear changes in the T_C and c/a ratio across the BST system. This local-structure behavior is typical for many solid solutions.

In contrast, Ca atoms in $Ba_{0.7}Ca_{0.3}TiO_3$ exhibit significant polar displacements ($z_{Ca} = 0.036$, $z_{Ba} = 0.023$) and, therefore, enhance the polarization. Fig. 6 illustrates the effective local $[CaO_{12}]$ coordination in $Ba_{0.7}Ca_{0.3}TiO_3$ obtained using the parameterized fits of the partial Ca-O PDF (Fig. 6(a)) determined from the RMC refinements. Calcium atoms are displaced along $\approx \langle 111 \rangle$ directions (Fig. 6(b)) toward the three O atoms that form a face of the $[TiO_6]$ octahedron. The three shortest Ca-O distances (2.54 Å, $\times 2$; 2.59 Å) are still significantly longer than those in $CaTiO_3$ (2.40 Å, $\times 4$) and, therefore, Ca atoms in $Ba_{0.7}Ca_{0.3}TiO_3$ are strongly under-bonded with a BVS of only ≈ 1.4. The average Ca-O and Ba-O distances (2.8 Å) are similar (Fig. 6(a)), with a BVS value for Ba of ≈ 3; that is, the Ba-O bonds are even more compressed relative to those in BT and BST. ($Ba_{1-x}Ca_xTiO_3$ solid solutions with $0 < x < 0.3$ yield similar Ca EXAFS data,[28] consistent with the analogous Ca coordination for this entire x-range). Remarkably, the trends for the local V_{oct} and δ_{Ti} in the $[TiO_6Ba_{8-N}Ca_N]$ groups are inverted relative to those in $Ba_{0.8}Sr_{0.2}TiO_3$ (Fig. 5(a)): the $[TiO_6]$ octahedra expand and δ_{Ti} values increase with increasing N. Thus, in BCT, Vegard's law is fulfilled (approximately) (Fig. 1(a)) at the expense of abnormal tensile and compressive *local* strain for the Ca-O and Ba-O bonds, respectively. The unusual behavior of local V_{oct} and δ_{Ti} (Fig. 5(a)) is caused by the oxygen displacements that mitigate this strain. In the absence of octahedral rotations (not even local), which in BCT are hindered by the compressed Ba-O bonds, an extent of strain relaxation around Ca is limited because deformation of the relatively rigid $[TiO_6]$ octahedra is required. Presumably, the energetic cost of this deformation outweighs the elastic energy associated with the strained Ca-O and Ba-O bonds. The unusually large bond strain and the associated anomalous BVS values for the Ca and Ba cations are consistent with the extensive miscibility gap in BCT.[9] The local Ti off-centering in both $Ba_{0.8}Sr_{0.2}TiO_3$ and

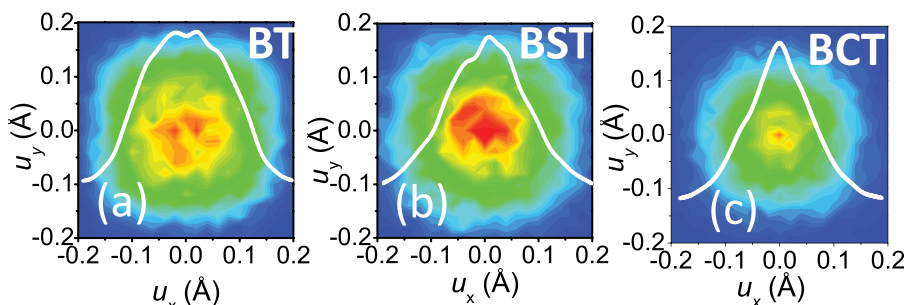FIG. 4. Maps of the (001)-projections of Ti PDD in (a) BT, (b) $Ba_{0.8}Sr_{0.2}TiO_3$, and (c) $Ba_{0.7}Ca_{0.3}TiO_3$. The PDD profiles (white traces) along the $\langle 110 \rangle$ directions are superimposed (the scale for these profiles is $\sqrt{2}u_x$).
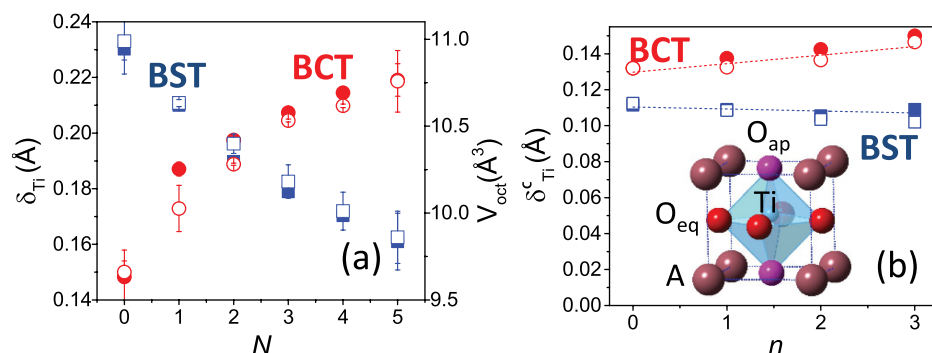
FIG. 5. (a) Dependence of the local V_{oct} (open symbols) and δ_{Ti} values (filled symbols) on the number (N) of Sr (blue) or Ca (red) atoms for the [$TiO_6Ba_{8-N}Sr_N$] and [$TiO_6Ba_{8-N}Ca_N$] clusters in $Ba_{0.8}Sr_{0.2}TiO_3$ and $Ba_{0.7}Ca_{0.3}TiO_3$, respectively. The error bars correspond to a single standard deviation determined from averaging over eight independently refined configurations. (b) Dependence of the c-axis component of δ_{Ti} (i.e., relative to O_{ap}) on the number (n) of the short O_{eq}-Sr (<2.65 Å) and O_{eq}-Ca (<2.55 Å) distances in the most frequent coordination groups [$TiO_6Ba_{8-N}Sr_N$] ($N = 2, 3$) (squares, blue) and [$TiO_6Ba_{8-N}Ca_N$] ($N = 2, 3$) (circles, red), respectively. A schematic rendering of the [$TiO_6Ba_{8-N}A_N$] (A = Sr, Ca) coordination group is shown as an inset.

$Ba_{0.7}Ca_{0.3}TiO_3$ increases as the corresponding V_{oct} increases (Fig. 5(b)). However, even at the individual unit-cell level, for a given V_{oct}, the off-centering is stronger in $Ba_{0.7}Ca_{0.3}TiO_3$ (Fig. 5(b)).

The positive effect of Ca on the local Ti off-centering resembles that of Pb in $PbTiO_3$.[28] $BaTiO_3$ and $PbTiO_3$ are examples of similar-volume perovskites that exhibit markedly different values of the tetragonal distortion and polarization (e.g., the short Ti-O bond in $PbTiO_3$ is 1.76 Å as opposed to 1.91 Å in $BaTiO_3$). Cohen[29] attributes this difference to the strong Pb off-centering accompanied by the formation of the covalent short Pb-O bonds (with equatorial O atoms), which stabilize a large tetragonal distortion that couples to the Ti displacements.[27] Additionally, significant hybridization in the short Pb-O bonds promotes larger displacements of Ti toward the apical oxygen atoms.[28] Our results suggest a similar mechanism for the enhancement of the local Ti off-centering in BCT. For example, formation of short bonds between Ca and the equatorial O atoms amplifies δ_{Ti} along the c-axis (Fig. 5(b), Fig. 6(b)); the contribution of this additional off-centering ($\approx$0.02 to 0.03 Å) to P_s ($\approx$0.04 to 0.06 C/m^2) is comparable to the enhancement of the A-site contribution caused by Ca displacements (Table I). No such effect is observed in BST (Fig. 5(b)).

In summary, we demonstrate that the sustained polarization and Curie temperature in BCT result from Ca displacements that contribute to polarization both directly and by enhancing the Ti off-centering. These positive contributions compete with the negative effect of the reduced average octahedral volume on Ti displacements, as reflected in the broad maximum in T_c (Fig. 1(b)). The BCT solid solutions exhibit severe bond strain. In particular, the oxygen coordination environments around Ca undergo only a limited relaxation, leaving the Ca atoms under-bonded. This local bond strain promotes ferroelectric Ca displacements, which also amplify the off-centering of Ti cations nearest to the Ca sites via a mechanism reminiscent of the effect of Pb in $PbTiO_3$. In contrast, in BST, the bonding requirements for the Sr atoms are nearly satisfied via the approximately isotropic relaxation of the [SrO_{12}] coordination units. Thus, the decline in polarization with increasing Sr concentration is caused entirely by the reduced Ti off-centering, as expected from intuitive ion-size/volume arguments. A conclusive comparison of structural behavior in BCT and BST solid solutions was enabled by the multiple-technique refinements, which provide unprecedentedly detailed and consistent description of the local and average atomic displacements.
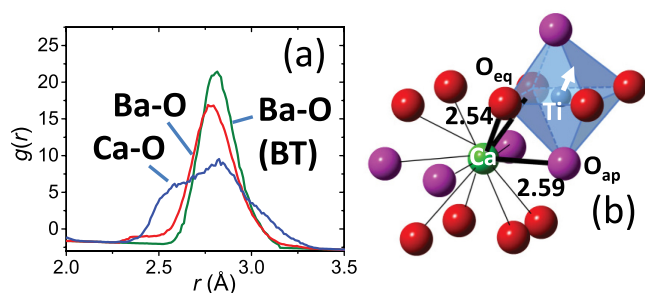
FIG. 6. (a) Partial Ca-O (red) and Ba-O PDFs (blue) in $Ba_{0.7}Ca_{0.3}TiO_3$ and partial Ba-O PDF (green) in $BaTiO_3$ as obtained from RMC refinements. (b) A schematic rendering of the effective [CaO_{12}] coordination obtained by fitting the parameterized model, which allows for rotation of displacements in the (110) plane, to the partial Ca-O PDF. The three shortest Ca-O distances are indicated using bold black lines. The Ti off-centering in the adjacent [TiO_6] octahedra that incorporate oxygen atoms featuring the shortest O-Ca bonds is enhanced (also Fig. 5(b)).

[1] M. E. Lines and A. M. Glass, *Principles and Applications of Ferroelectrics and Related Materials* (Oxford University Press, Oxford, 1977).

[2] H. D. Megaw, *Crystal Structures: A Working Approach* (W. B. Saunders, Philadelphia, 1973).

[3] G. H. Kwei, A. C. Lawson, S. J. L. Billinge, and S.-W. Cheong, J. Phys. Chem. **97**, 2368–2377 (1993).

[4] R. Comes, M. Lambert, and A. Guinier, Solid State Commun. **6**(10), 715–719 (1968).

[5] B. Ravel, E. A. Stern, R. I. Vedrinskii, and V. Kraizman, Ferroelectrics **206**, 407 (1998).

[6] B. D. Ravel, "Ferroelectric phase transitions in oxide perovskites studied by XAFS," Ph.D. dissertation (University of Washington, 1997).

[7] R. D. Shannon, Acta Crystallogr., Sect. A: Cryst. Phys., Diffr., Theor. Gen. Crystallogr. **32**, 751–767 (1976).

[8] J. A. Basmajian and R. C. DeVries, J. Am. Ceram. Soc. **40**(11), 373–376 (1957).

[9] R. C. DeVries and R. Roy, J. Am. Ceram. Soc. **38**(4), 142–146 (1955).

[10] V. V. Lemanov, E. P. Smirnova, P. P. Syrnikov, and E. A. Tarakanov, Phys. Rev. B **54**(5), 3151–3157 (1996).

[11] T. Mitsui and W. B. Westphal, Phys. Rev. **124**(5), 1354–1359 (1961).

[12] D. Fu, M. Itoh, S.-y. Koshihara, T. Kosugi, and S. Tsuneyuki, Phys. Rev. Lett. **100**, 227601 (2008).

[13] V. A. Isupov, Fiz. Tverd. Tela **29**(11), 3487 (1987).

[14] J. P. Itié, B. Couzinet, A. Polian, A. M. Flank, and P. Lagarde, Europhys. Lett. **74**(4), 706–711 (2006).

[15] Ph. Pruzan, D. Gourdain, J. C. Chervin, B. Canny, B. Couzinet, and M. Hanfland, Solid State Commun. **123**(1), 21–26 (2002).

[16] See supplementary material at http://dx.doi.org/10.1063/1.4802996 for details of sample synthesis and characterization.

[17] The solubility limit for Ca at 1450 °C has to be higher than that reported previously,[9] since our $Ba_{0.7}Ca_{0.3}TiO_3$ sample is single-phase.

[18] A. C. Larson and R. B. von Dreele, "General structure analysis system," Los Alamos National Laboratory Report LAUR, 1994.

[19] W. Zhong, R. D. King-Smith, and D. Vanderbilt, Phys. Rev. Lett. **72**(22), 3618–3621 (1994).

[20] V. Krayzman, I. Levin, J. C. Woicik, D. Yoder, and D. A. Fischer, Phys. Rev. B **74**(22), 224104 (2006).

[21] M. G. Tucker, D. A. Keen, M. T. Dove, A. L. Goodwin, and Q. Hui, J. Phys. Condens. Matter **19**(33), 335218 (2007).

[22] V. Krayzman, I. Levin, J. C. Wocik, T. Proffen, T. A. Vanderah, and M. G. Tucker, J. Appl. Crystallogr. **42**, 867–877 (2009).

[23] V. Krayzman and I. Levin, J. Appl. Crystallogr. **45**, 106–112 (2012).

[24] For example, refinements without EXAFS yielded partial PDFs Ca-O and Sr-O that were incompatible with the corresponding experimental EXAFS data. Performing the same refinements under bond-valence-sum[25] constraints for Ca and Sr also produced grossly incorrect Ca-O and Sr-O partial PDFs that did not match the EXAFS. Determination of the correct Ca-O and Sr-O partial PDFs from the total scattering alone is virtually impossible because of their small contributions to the respective total PDFs and a complete overlap of the A-O (A = Ba, Sr, Ca) and O-O partials. Refinements using all of the powder data alone (i.e., total scattering, Bragg intensities, EXAFS) could not reproduce the patterns of diffuse scattering in electron diffraction: The resulting configuration lacked the appropriate correlations of Ti and O displacements, which are a critical attribute of the local structure in $BaTiO_3$ and its solid solutions. Importantly, the inability to reproduce these extended (several nanometers) correlations resulted in the incorrect probability density distributions for all the atoms because $\sigma_{ij}^2 = \sigma_i^2 + \sigma_j^2 - 2\phi\sigma_i\sigma_j$, where σ_{ij} is the Debye-Waller factor for the distance between atoms i and j, σ_i and σ_j are the Debye-Waller factors for these atoms, and ϕ is the correlation parameter (positive for the parallel displacements of atoms i and j and negative for the antiparallel displacements). Thus, including the diffuse scattering patterns in the fit was critical for obtaining the correct structural models. Similar arguments apply to other data.

[25] The angles between the Ti displacements and c-axis were determined using the mid-point between the apical oxygen atoms as a reference.

[26] I. D. Brown and D. Altermatt, Acta Crystallogr., Sect. B: Struct. Sci. **41**, 244–247 (1985).

[27] An ideal BVS value for divalent Ca, Sr, and Ba, is 2. This BVS value corresponds to strain-free metal-oxygen bonds. Deviations from the ideal BVS indicate either tensile (<2) or compressive (>2) bond strain.

[28] V. Krayzman, I. Levin, J. C. Woicik, F. Bridges, E. J. Nelson, and D. C. Sinclair, J. Appl. Phys. **113**, 044106 (2013).

[29] R. E. Cohen, Nature **358**(6382), 136–138 (1992).